

Isoform-specific upregulation of FynT kinase expression is associated with tauopathy and glial activation in Alzheimer's disease and Lewy body dementias

Clara Y.B. Low^{1^}, Jasinda H. Lee^{2^}, Frances T.W. Lim¹, Chingli Lee¹, Dag Aarsland³, Clive Ballard⁴, Paul T. Francis^{4,5}, Mitchell K.P. Lai^{2, 5*}, Michelle G.K. Tan^{1,2*}

¹Department of Clinical Research Singapore General Hospital, Outram, Singapore

²Department of Pharmacology, Yong Loo Lin School of Medicine, Kent Ridge, Singapore

³Department of Old Age Psychiatry, Institute of Psychiatry, Psychology and Neuroscience, King's College London, London, UK

⁴Institute for Health Research, University of Exeter Medical School, Exeter, UK

⁵Wolfson Centre for Age-Related Diseases, King's College London, London, UK

[^]These Authors contributed equally to the manuscript

***Corresponding Authors:**

Mitchell K.P. Lai, PhD, Department of Pharmacology, Yong Loo Lin School of Medicine, National University of Singapore, Unit 09-01, Centre for Translational Medicine (MD6), 14 Medical Drive, Kent Ridge, Singapore 117599.

mitchell.lai@dementia-research.org

Michelle G.K. Tan, PhD, Department of Clinical Translational Research, Singapore General Hospital, The Academia, Level 9, Discovery Tower, 20 College Road, Singapore 169856.

michelle.tan.g.k@sgh.com.sg

DR MITCHELL KP LAI (ORCID ID: 0000-0001-7685-1424)

DR MICHELLE GK TAN (ORCID ID: 0000-0002-3203-2023)

Keywords: Alzheimer's disease; Lewy body dementia; Fyn kinase; Alternative splicing; Tau; Glial activation

ABSTRACT

Cumulative data suggest the involvement of Fyn tyrosine kinase in progression of Alzheimer's disease (AD). Previously, our group has shown increased immunoreactivities of the FynT isoform in AD neocortex (with no change in the alternatively spliced FynB isoform) which associated with neurofibrillary degeneration and reactive astrogliosis. Since both the aforementioned neuropathological features are also frequently found in Lewy Body dementias (LBD), we investigated potential perturbations of Fyn expression in the postmortem neocortex of patients with AD, as well as those having one of the two main subgroups of LBD: Parkinson's disease dementia (PDD) and dementia with Lewy bodies (DLB). We found selective upregulation of FynT expression in AD, PDD and DLB which also correlated with cognitive impairment. Furthermore, increased FynT expression correlated with hallmark neuropathological lesions, soluble β -amyloid and phosphorylated tau, as well as markers of microglia and astrocyte activation. In line with the human postmortem studies, cortical FynT expression in aged mice transgenic for human P301S tau was upregulated and correlated with accumulation of aggregated phosphorylated tau as well as with microglial and astrocytic markers. Our findings point to FynT being an important mediator of disease progression in neurodegenerative dementias, likely via effects on tauopathy and neuroinflammation.

(205 words)

INTRODUCTION

Alzheimer's disease (AD) and Lewy body dementias (LBD) are respectively the number one and two causes of neurodegenerative dementia in the elderly, and contribute to significant morbidity for both sufferers and their caregivers, as well as to global healthcare burden (3, 27, 61). LBD consists of two clinical subtypes: Parkinson's disease dementia (PDD) and dementia with Lewy bodies (DLB), where differentiation is mainly based on the "one-year rule" in which patients presenting with dementia before, or within a year of, parkinsonism symptoms are diagnosed as DLB, whereas dementia occurring > 1 year after parkinsonism is considered to be PDD (40). While PDD and DLB share similar neuropathological features, especially the presence of cortical aggregated α -synuclein-containing Lewy bodies (LB), significant differences in clinical presentation as well as neurochemical perturbations have been reported between them (2, 4, 16, 43, 58, 59), giving rise to ongoing debate on whether PDD and DLB are separate entities or part of the same spectrum of LBD (1, 29, 39, 54). Interestingly, in addition to LB, both PDD and DLB manifest variable burdens of hallmark AD lesions, namely intracellular amyloid plaques (AP) consisting mainly of insoluble, aggregated β -amyloid peptides ($A\beta$); and intercellular neurofibrillary tangles (NFT) formed from aggregation of hyperphosphorylated tau proteins into paired helical filaments (13, 18, 19, 23). Furthermore, the presence of chronic neuroinflammation and glial activation, which are intimately linked to both AP and NFT (33, 42), are also salient features of AD and LBD (9, 52). Therefore, studies focused on the pathophysiological mechanisms and effects of AP and NFT formation (51) should consider the applicability and implications of their findings to LBD.

Given the diverse biological functions (ranging from regulating brain function to modulating T-cell signaling) attributed to Fyn, a member of the Src family tyrosine kinases (50), it is perhaps unsurprising that Fyn kinase has been implicated in AD pathophysiology (20). As Fyn is alternatively spliced into two major isoforms: brain-predominant FynB and immune cells-predominant FynT, we have measured FynB versus FynT immunoreactivities in postmortem AD neocortex, and found selective increases in FynT which also associated with neurofibrillary degeneration and reactive astrogliosis (34). These findings are in line with *in-vitro* data showing that prolonged inflammatory response and activation in astrocytes are mediated by pro-inflammatory cytokine-induced FynT (35). However, the status of Fyn isoform expression as well as potential associations with neuropathological features and neuroinflammatory markers in LBD is currently unknown. In this study, we used a human transcriptome microarray approach to quantify Fyn isoform expression in neocortex of AD and LBD patients together with aged non-demented subjects, and correlated the measures with A β and phosphor-Tau concentrations, neuroinflammatory markers, neuropathological and clinical scores. To further study possible links between Fyn perturbations and NFT formation, we also monitored longitudinal changes of Fyn isoform expression in association with tau pathology and neuroinflammation in a transgenic mouse model of human tauopathy which harbors the human P301S tau mutation (60).

METHODS

Patients, clinical and neuropathological assessments

Post-mortem brain tissues from the frontal (Brodmann Area, BA9, dorsolateral / medial prefrontal cortex) and temporal (BA21: middle temporal gyrus) regions of subjects with AD, DLB, PDD, as well as elderly controls (CTRL) without neurological or psychiatric diseases were obtained from the University Hospital Stavanger, Newcastle Brain Tissue Resource, the London Neurodegenerative Diseases Brain Bank and the Thomas Willis Brain Collections at Oxford University, the UK sites being part of the Brains for Dementia Research network (<http://brainsfordementiaresearch.org.uk>). Subjects with dementia were part of longitudinal studies and were followed-up annually with clinical assessments including the Mini-Mental State Examination (MMSE)(15) to measure cognitive decline until death, at which time informed consent was obtained from next-of-kin before removal of brains. Consensus criteria used for clinical diagnoses of AD, DLB and PDD with neuropathologic confirmation have been previously described in detail (10). In addition, semi-quantitative scoring (0 = None, 1 = Sparse, 2 = Moderate and 3 = Abundant) of AP, NFT / neuropil threads, and LB / Lewy neurites as visualized by immunostaining with 4G8, AT8 and α -synuclein antibodies, respectively, were performed by neuropathologists blinded to clinical diagnosis as previously described (23). For the neurochemical and gene expression studies, 1 cm³ frozen brain chunks were obtained from BA9 and BA21 of the hemisphere contralateral to the one used for neuropathologic studies, then stored at -80°C before further processing for homogenate preparation and RNA isolation.

Brain tissues from transgenic mice

The P301S tau transgenic mouse line PS19 (B6N.Cg-Tg(Prnp-MAPT*P301S)PS19Vle/J, Stock no: 024841) were obtained from the Jackson Laboratory (Bar Harbor, ME, USA) and bred with wild type (WT) control, C57BL/6NJ (stock no:005304) to generate hemizygotes and WT littermate controls. The strain harbours the 1N4R isoform of human MAPT gene with the P301S mutation, driven by mouse prion protein promotor which expressed the human P301S tau at levels 5-fold higher than endogenous mouse tau (60). Brains from both genotypes were harvested directly after CO₂ euthanasia before 6 months (mo) old (WT: n=13, 8M/5F, 4.9±0.2 mo; P301S: n=13, 6M/7F, 4.7±0.2 mo) and after 6 months old (WT: n=18, 10M/8F, 8.6±0.4 mo; P301S: n=18, 9M/9F, 8.9±0.4 mo). After removing cerebellum, olfactory bulb, and meninges, the cortex were separated into left and right hemispheres for RNA isolation and brain homogenate preparation, respectively.

Brain tissue processing

Unless otherwise specified, all chemicals and reagents were purchased from Sigma Aldrich (St Louis, MO, USA) and of analytical grade. Frozen human brain chunks from BA9 and BA21 were thawed on ice, dissected free of meninges and white matter, then homogenized (10 s, maximum speed) with an Ultra-Turrax® T-25 homogenizer (IKA-Werke, Staufen, Germany) in ice-cold buffer (50 mM Tris-HCl, 120 mM NaCl, 5 mM KCl, pH 7.4) with cOmplete™ protease inhibitor cocktail and PhosSTOP™ phosphatase inhibitor tablets (Roche Life Science, Penzberg, Germany). Brain homogenates from mice were prepared as above without the prior dissection step. For both human and mice brains, representative portions were kept in TRIzol® reagent (Invitrogen Inc., Carlsbad, CA, USA) at -80°C for subsequent RNA extraction.

Enzyme-linked immunosorbent assays (ELISA) of pS396 Tau and soluble A β 42 in human neocortex

Aliquots of brain homogenates was treated with 5M Guanidine for detection of tau with serine phosphorylation at position 396 (pS396 Tau) by ELISA according to manufacturer's instructions (KHB7031, ThermoFisher Scientific, Waltham, MA, USA). Separate homogenate aliquots were agitated using a sonicator for 30 mins at 4 °C before centrifugation at 6,000 g, 30 min at 4 °C, with the supernatant used for detection of soluble A β ₁₋₄₂ peptides (sA β 42) by ELISA according to manufacturer's instructions (KHB3441, ThermoFisher Scientific). Concentrations values in pg/mL were normalized to protein content of each sample (determined using Pierce Coomassie Plus Reagent, ThermoFisher Scientific) and presented as pg/mg protein.

mRNA isolation, reverse transcription, real-time polymerase chain reaction (RT-PCR) and capillary electrophoresis

Brain tissue kept frozen in TRIzol[®] reagent (Invitrogen Inc., Carlsbad, CA, USA) were thawed and processed for RNA extraction following manufacturer's instructions. A Fragment Analyzer[™] system (Advanced Analytical Technologies Inc, Ankeny, IA, USA) was used for evaluating RNA quality, with RQN <3.0 excluded from further analysis. 2 μ g of RNA was reverse-transcribed to cDNA using High-Capacity cDNA RT kit (Applied Biosystems, Foster City, CA, USA) in accordance to manufacturer's protocol. Semi-quantitative measurements of gene expression were performed on the 7500 Fast Real-time PCR system (Applied Biosystems) or CFX96[™] Real-time PCR system (Biorad) using GoTaq[®] qPCR Master Mix (Promega, Madison, WI, USA). The primer

sequences used in this study are listed in **Supplementary Table S1**. All real-time RT-PCR assays were performed in duplicate. Standard curves of each gene were generated independently by 10x serial dilution of template DNA. The relative signal intensity of each sample was calculated according to the corresponding standard curve. Normalization was performed in each sample by dividing the relative signal intensity of gene of interest to geometric mean of β -actin, GAPDH and 18S rRNA. To determine FynT to FynB ratios using capillary electrophoresis, a pair of common primers spanning the alternative spliced exon of Fyn were used as described previously (34). Peak areas of FynT (219bp DNA amplicon) and FynB (228bp DNA amplicon) in each electropherogram were translated into expression level and used to determine ratios of FynT to FynB expression.

Human Transcriptome Array (HTA) data and Gene Ontology (GO) term enrichment analyses

A subset of samples (9 CTRL, 9 AD, 12 DLB, 12 PDD) from BA9 were processed for high-throughput transcriptome profiling using the GeneChip[®] HTA 2.0 array (Affymetrix, Santa Clara, CA, USA). The dataset has been deposited with the Gene Expression Omnibus (GEO) and will be accessible ([Access #](#)). Using the Gene View module of Partek Genomics Suite[®] 7.0 software (Partek Inc, St Louis, MO, USA), we were able to allocate differentially expressed probesets to specific transcript variants of Fyn. Expressed probesets which were significantly correlated with the FynT-specific probesets (PSR06025242.hg.1) at false discovery rate (FDR)(5) cutoff of 5% were retrieved. Genes with ≥ 10 representative probesets that consistently correlated with FynT were subject to Gene Ontology (GO) term enrichment analyses

using DAVID Bioinformatics Resources 6.7 (<http://david.abcc.ncifcrf.gov/>) (26), with Benjamini's enrichment *p*-values adjustment for multiple testing using FDR of 5% (24, 25). For this study, we focused on GO categories of Biological Processing and Cellular components, after removing general GO terms with enrichment factor <2.

Homogenous Time-Resolved Fluorescence (HTRF) assays of mouse brain

homogenates

Cisbio® HTRF assays (PerkinElmer Inc. Waltham, MA, USA), a technology combining standard fluorescence resonance energy transfer (FRET) with time-resolved measurement of fluorescence, were used for measuring total human tau protein (MAP-Tau Kit), phosphorylated tau (Phospho-Ser202/Thr205 human TAU kit) and aggregated tau (Tau aggregation kit) according to manufacturer's instructions. A portion of the right hemisphere was homogenized in Cisbio lysis buffer with blocking reagent using 5 mm stainless steel beads in a TissueLyser LT (Qiagen, Venlo, the Netherlands) tissue disruptor (two rounds of 50 Hz, 2 min). After centrifugation at 21,000 g for 20 min at 4°C, supernatants were measured for protein concentration using the Bradford protein assay kit (BioRad, Hercules, CA, USA). Equal amounts of brain homogenate were then diluted and incubated with respective antibodies for 24 h at room temperature. Samples were excited at 340 nm and emission values collected at 620 nm (Donor) and 665 nm (Acceptor) using EnSpire® multimode plate reader (Perkin Elmer). For data analysis, HTRF ratio was calculated for each individual well by the ratio of the two emission values (Signal 665 nm/ Signal 620 nm) and multiplied by 10,000 to ease data processing. Data were presented as Delta F%

which reflected the signal to background of the assay, and calculated as [HTRF ratio (sample) - HTRF ratio (negative control)] / HTRF ratio (negative control) x 100.

Statistical analyses

Pair-wise differences amongst groups were analyzed by Kruskal-Wallis analysis of variance (ANOVA) with *post-hoc* Dunn's test or data transformed to log₂ base value and analyzed using one-way ANOVA with Bonferroni's *post-hoc* tests. Pearson's or Spearman's correlations was used to for parametric or non-parametric variables, respectively. For all analyses, two-tailed *p*-values of < 0.05 were considered to be statistically significant. Statistical analyses and plotting of graphs were performed using the PRISM Version 5 software (GraphPad, San Diego, CA, USA).

RESULTS

Demographic and disease variables of the study cohort

Table 1 shows the maximum available numbers of aged controls (CTRL) as well as a community-based cohort of PDD, DLB and AD patients. Groups were not significantly different in age at death and postmortem interval (one-Way ANOVA *p* > 0.05).

Within the dementia subgroups (AD, PDD and DLB), no significant difference in dementia severity (indicated by MMSE decline per year) was observed (Kruskal-Wallis ANOVA *p* > 0.05). Braak staging (7) for extent of AD pathological changes showed all but one of the aged CTRL in Braak stage ≤ II, with one in III-IV (another four CTRL did not have Braak staging data). In contrast, ten out of thirteen available AD cases were Braak V/VI, with the rest in Braak III/IV. PDD and DLB showed variable AD pathology ranging from Braak ≤ II to V/VI, with DLB showing higher numbers of

those with more advanced stages compared to PDD. Furthermore, ELISA measures of soluble A β 42 and pS396Tau, used respectively as markers of amyloid and neurofibrillary tangle burden, were also raised in the dementia subgroups, with the highest levels in AD, and the lowest in PDD (**Table 1**). These neuropathological and biochemical features are in line with previous clinical and postmortem observations of AD and Lewy body dementias, especially with regards to PDD harbouring the lowest AD pathological burden amongst the dementia subgroups (19, 23).

Selective upregulation of FynT isoform expression in neocortex of AD and LBD

We have previously reported specific increases of FynT immunoreactivities which contrasted with unchanged brain-predominant FynB in AD (34). Here, using a high throughput gene profiling (HTA) platform, we found similar FynT upregulation in a separate cohort of AD and further extended this observation to DLB and PDD. **Figure 1** shows Gene View plot where probeset PSR06025242.hg.1 (indicated by blue asterisk) corresponding to sequence for FynT-specific exon was significantly up-regulated in AD (~3 fold), DLB (~2.5 fold) and PDD (~1.8 fold) prefrontal cortex compared with CTRL. In contrast, probesets corresponding to common exons and FynB-specific exons (yellow boxes in FynB transcript, **Figure 1**) showed no significant induction in the dementia subgroups. To confirm these findings, we determined the proportional amounts of FynB and FynT in two brain regions (BA9 and BA21) of aged CTRL and dementia subgroups using common primers spanning the alternative spliced exon of Fyn for RT-PCR followed by capillary electrophoresis. The representative electropherograms in **Figure 2A** indicated that the FynT peaks were about ten times lower than FynB peaks in CTRL, while elevations of FynT peaks

relative to FynB were detected in the dementia subgroups. Indeed, AD, DLB and PDD all had significantly higher FynT to FynB ratios compared to CTRL in both BA9 and BA21 (**Figure 2B**), with the ratios showing a high degree of correlation between the two brain regions (Pearson's $r = 0.79$, $p < 0.001$).

FynT upregulation correlated with cognitive impairment and neuropathological features in AD and LBD

In order to investigate potential associations between Fyn perturbations and clinical or neuropathologic features, FynT and FynB expression levels were determined by real-time RT-PCR and correlated with predeath MMSE, neuropathologic scores as well as A β 42 and pS396 Tau concentrations. Consistently, FynT was observed to be upregulated in the dementia subgroups, reaching statistical significance for AD and DLB (with a trend towards increase for PDD) in BA9, and for all three dementia subgroups in BA21 (**Figure 3A** left panel). We also confirmed that FynB expression were not significantly altered in the dementia subgroups (**Figure 3A** right panel).

Figure 3B shows that FynT expression in both BA9 and BA21 negatively correlated with predeath MMSE scores in the combined dementia cohort, suggesting that FynT upregulation may be associated with more severe cognitive impairment.

Furthermore, **Figure 3C** lists the correlation coefficients between Fyn expression and (i) semi-quantitative scores of amyloid plaques, neurofibrillary tangles (NFT), Lewy bodies (LB) and combined neuropathologic scores (which we have previously shown to be variably increased in LBD (23)); (ii) Braak staging and (iii) concentrations of soluble A β (sA β 42) and phosphorylated Tau (pS396 Tau). Interestingly, FynT expression was widely correlated with the neuropathological scores (NFT, LB and

combined scores), Braak stage, sA β 42 and pS396 Tau measures, especially in BA9, while FynB did not correlate with neuropathologic scores and biochemical measures except for Braak stage and pS396 Tau in BA9 (**Figure 3C**). Taken together, our data suggest that FynT isoform-specific upregulation in the neocortex may be associated with clinical severity and neuropathological burden in AD and LBD.

FynT upregulation correlated with markers of neuroinflammation in AD and LBD

We have previously found that FynT induction was associated with astrocyte activation under neuroinflammatory conditions (35). In PD, microglial activation was also reported to be dependent on Fyn kinase activity (47). Here, we investigated potential associations between Fyn expression and neuroinflammatory responses using glial fibrillary acidic protein (GFAP) and CD11b expression to indicate astrogliosis and microglial activation respectively (14, 38). **Figure 4A** shows increased GFAP expression in BA9 for AD, and in BA21 for DLB, while expression remained unchanged for PDD in both regions (left panel). For microglia marker CD11b, expression was significantly increased in BA9 for AD, and in BA21 for all dementia subgroups (right panel). **Figure 4B** indicates that FynT expression correlated with both GFAP and CD11b in both brain regions in the combined cohort. To study potential sources of Fyn isoform expression in brain, we measured FynT to FynB ratios in isolated rat primary astrocyte, microglia and neurons and confirmed higher FynT expression in both microglia (0.858 ± 0.150) and astrocytes (0.343 ± 0.042) compared with neurons (0.068 ± 0.011 , see **Supplement Figure S1**). Taken together, our results suggested that FynT induction may play a role in astrogliosis and microglial activation in AD and LBD neocortex.

Synaptic dysfunction is a potential consequence of FynT upregulation in AD and LBD

To investigate the potential pathophysiological impact of FynT induction in neurodegenerative dementias, we utilized the high-throughput transcriptome profiling data on BA9 of a subset of the cohort (9 CTRL, 9 AD, 12 DLB, 12 PDD). Stringent criteria (see details in methodology) were set to identify candidate genes which were correlated either positively or negatively with FynT. In summary, 515 FynT-positively correlated genes and 1437 FynT-negatively correlated genes were uncovered and independently analyzed by DAVID (26) to gain an overview of the functional profiles of associated genes in order to understand the underlying processes. **Table 2** summarizes the top 5 GO (gene ontology) terms found in each category (the full list of GO terms and corresponding genes can be found in **Supplementary Table S2**). In general, genes positively-correlated with FynT were mainly associated with cell adhesion, whereas the negatively-correlated genes were associated with neuronal function and components found in dendrites and synapses (**Table 2**). These results suggest that synaptic dysfunction and synaptopathology may be associated with FynT upregulation in AD and LBD.

Selective upregulation of FynT is associated with tauopathy and neuroinflammation in aged P301S mice

Finally, the potential pathophysiological links between FynT induction, tau pathology and neuroinflammation were studied in a P301S Tau transgenic mouse model of tauopathy at two age groups: < 6 mo when there is minimal brain pathology; and ≥ 6

mo, when the mice are known to manifest neurofibrillary tangles and neuroinflammation during disease progression. HTRF assays confirmed that P301S Tau mice expressed high levels of human tau in the brain when compared with wildtype (WT) littermate controls at both age groups (**Figure 5A**, left panel). However, the younger P301S mice (< 6 mo) showed minimal phosphorylated tau and aggregation, similar to WT (**Figure 5A**, middle and right panels). In contrast, older mice (≥ 6 mo) showed significantly increased levels of phosphorylated, aggregated tau (**Figure 5A**, middle and right panels). Similar to observations of the human postmortem brains, we found significantly increased FynT expression as well as higher FynT to FynB ratio in older, but not younger, P301S mice (**Figure 5B** left and right panels), whilst FynB expression was unchanged in both age groups (**Figure 5B** middle panel). Furthermore, markers of neuroinflammatory responses as indicated by GFAP and CD11b expression were significantly increased only in older P301S mice (**Figure 5C**). Lastly, **Figure 5D** lists the correlation coefficients between expression of Fyn isoforms, GFAP and CD11b as well as HTRF measurements of phosphorylated and aggregated Tau, and showed that both FynT and FynT:FynB correlated with the neuroinflammatory markers as well as pathologic Tau markers. Therefore our findings suggest that selective FynT upregulation likely occurs downstream of tauopathy and is associated with disease progression, including neuroinflammation, in P301S mice.

DISCUSSION

FynT kinase as the mediator of A β -associated tauopathy and neuroinflammation

Whilst processes associated with amyloid precursor protein mismetabolism leading to accumulation of insoluble A β have well-established roles in AD pathogenesis (49), it is the hyperphosphorylation of tau and ensuing formation of neurofibrillary tangles (NFT) which correlated more closely with disease progression, and may indeed mediate the clinical severity of AD (6, 44). As NFT (together with amyloid plaques) are a common feature of both AD, PDD and LDB, these neurodegenerative dementias can be defined as tauopathies. In this paper, we reported further evidence for a selective-upregulation of the FynT isoform in AD neocortex, and extended these observations to PDD and LDB. As basal FynT expression was around one tenth of FynB expression in the brain (see **Figure 2**), we speculate that the inability of some previous studies to detect Fyn induction in AD (31, 32) was likely due to the use of non isoform-specific measurements, since the amount of FynT increase would likely be masked by the unchanged, predominant FynB isoform. Importantly, we showed here that FynT upregulation was associated with astrogliosis, microglial activation, neuropathologic burden and dementia severity, therefore suggesting, as others have (20), that Fyn may mediate the pathophysiological link between amyloid and tau. Indeed, Fyn can regulate A β -induced excitotoxicity by interacting with dendritic tau, the latter targeting Fyn postsynaptically to glutamate NMDA receptors where excitotoxic signals are transmitted (28). A β -induced tau accumulation at somatodendritic compartments was also found to be Fyn-dependent (37). In another study, binding of A β oligomers to postsynaptic prion proteins was shown to trigger Fyn-mediated signaling cascades

leading to tauopathy and synaptotoxicity (55, 57). Fyn has also been reported to mediate NF- κ B signaling as well as microglial and inflammasome activation in PD (47, 48). Furthermore, Fyn directly phosphorylates Tau and may contribute to NFT burden (36). On top of these observations, we previously reported strong associations between NFT burden and increased FynT immunoreactivity in AD (34). Taking into consideration the present data, we postulate that at least some of the pathogenic mechanisms mentioned above may be mediated by altered regulation of alternative splicing which favours FynT.

Potential mechanisms of FynT-associated neuronal dysfunction in AD and LBD

Several studies have demonstrated that Fyn kinase can modulate synaptic plasticity and learning (11, 12, 30, 53). In this study, we speculate that FynT upregulation-associated synaptic dysfunction may adversely impact dementia progression based on the consistent negative correlations of FynT with genes coding for functional components of neurons and synapses (**Table 2**), as well as with predeath cognitive scores (**Figure 3B**). Recently, mutant P301L tau has been shown to promote aberrant Fyn nanoclustering in dendritic spines which likely contributes to synaptic dysfunction (46). In this study, we used mutant P301S tau mice to demonstrate that age-dependent increment of phosphorylated and aggregated tau was associated with FynT upregulation (**Figure 5**). Tau pathology has been suggested to contribute to development of chronic inflammatory responses involving reactive astrogliosis (41). We have reported increased FynT immunoreactivity in hypertrophic cytoplasm of reactive astrocytes in the AD brain (35), which is corroborated here by the finding of significant correlations between FynT and GFAP expression (**Figure 4B**).

Additionally, Fyn induction in post-mortem PD brains has been reported to be associated with neuroinflammatory responses resulting from microglial activation (48). Interestingly, the present *in-vitro* data indicate the highest expression of FynT in microglia, followed by astrocyte, whilst neurons had the lowest expression (**see Figure S1**). As the correlation coefficient for FynT and CD11b expression was higher than those between FynT and GFAP or pS396Tau in the postmortem study, our data suggest FynT upregulation in the AD and LBD brain could be due in large part to activation of predominantly FynT-expressing microglia, which may in turn contribute to chronic neuroinflammation-associated neuronal damage (21). However, given the significant (albeit weaker) correlations between FynT and GFAP, as well as previously reported localization of FynT in reactive astrocytes (34), we postulate that astrogliosis underlies at least part of the observed FynT upregulation. Here, it is worth noting that FynT likely plays a critical role in astrocyte activation, as we have previously shown that neuroinflammatory responses to tumor necrosis factor is abolished in astrocytes expressing a kinase-dead mutant of FynT (35). Therefore, when considered in the context of previous studies, our current *in-vitro* and postmortem data suggest that in AD and LBD, FynT upregulation occurs downstream of tau phosphorylation and NFT formation, and is involved in astrocyte and / or microglial activation, leading in turn to neuroinflammation-associated synaptic dysfunction and neuronal damage.

Isoform-specific role of FynT as therapeutic target for neurodegenerative dementia

Fyn kinase has already been proposed as a potential therapeutic target for AD (45).

In this regard, a previous study showed that targeting Fyn in an AD mouse model

restored synaptic density, limited tau aggregation, reduced microglial activation and subsequently reversed memory deficits without attenuating A β load (30). However, it is worth noting that AZD0530, the Src family kinase inhibitor used in the animal study, showed no statistically significant improvement on neuroimaging outcome when compared with placebo in a year-long Phase IIa clinical trial (although a trend towards less shrinkage of the hippocampus and entorhinal cortex was observed in the treated group)(56). One insight that may be gleaned from our study is the need to refine the target to Fyn, and specifically the FynT isoform, for potentially improved efficacy as well as reduced off-target adverse effects, since the major brain variant FynB has important physiological functions and should not be targeted. Furthermore, when a FynT-specific compound does become available, our data suggest extending assessments of their clinical utility to LBD in addition to AD.

Study Limitations

There are several limitations apparent in this study which are related to the limited number of available samples. Therefore, in interpreting findings where changes are found in one, but not both of the brain regions examined (for example, significant correlation between FynT and NFT scores in BA9 prefrontal cortex but not BA21 temporal cortex, see **Figure 3C**), it is unclear whether the observed regional differences has a genuine pathophysiological basis or was due to higher data variability in BA21 resulting in non-significance of the association. On the other hand, FynT expression seemed to be increased in both regions in LBD, but did not reach statistical significance in BA9 for PDD (**Figure 3A**). Whilst higher AP and NFT loads are detected in DLB compared with PDD (22, 29), and NFT (which we have shown here to

be strongly correlated with FynT) is known to originate from the enthorhinal, hippocampal and neocortical regions of the temporal lobe followed by progression into the prefrontal and other neocortical areas (8), we cannot at present confirm whether these regional differences are DLB- or PDD-specific due to associations with pathological burden, necessitating follow-up studies on larger cohorts looking at multiple brain regions.

Secondly, the current study has not studied Fyn associations with LBD-specific lesions (α -synuclein-containing Lewy bodies, LB) in detail. While the focus of our study has been on AD pathological features which are present in both AD and LBD, FynT may also be linked to LB, as suggested by **Figure 3C**. However, it is at present unclear whether, or how, FynT may be related to α -synuclein aggregation and related pathophysiology *per se*, as assays of soluble α -synuclein revealed similar baseline cortical concentrations across controls and dementia subgroups which did not correlate with Fyn or other neuropathological measures (data not shown). These negative findings suggest that other potentially pathogenic species of α -synuclein, e.g., Ser129-phosphorylated α -synuclein (17) need to be measured in follow-up studies of potential Fyn involvement in LBD-specific pathology.

Finally, the current study employed a genomics approach with the use of microarrays and RT-PCR to study Fyn expression and associations with a wide range of gene expression changes. There is therefore a lack of histological and cellular localization data, which is mitigated somewhat by i) the use of primary cultures to provide *in-vitro* validation of the likely sources of FynT, namely, astrocytes and microglia (**Supplementary Figure S1**); and (ii) our previous study which showed the

localization of FynT in activated astrocytes in AD (34). However, follow-up studies are needed to confirm the findings for microglia and also extend them to LBD.

CONCLUSION

Using microarray platforms, we report FynT-isoform specific upregulation in the neocortex of AD, DLB and PDD. The observed induction of FynT was closely associated with tauopathy and neuroinflammation, and may mediate their deleterious effects on synaptic and cognitive functions. In corroboration, age-dependent FynT upregulation was detected in P301S mutant tau transgenic mice, which was significantly correlated with phosphorylated and aggregated tau, as well as with markers of microglial and astrocytic activation. Our findings point to FynT as the pathogenic Fyn isoform for AD and LBD, and propose a refinement of therapeutic approach from non-specific inhibition of Src family kinases to a more focused search for compounds which specifically target FynT as potential treatment for AD-related chronic neuroinflammation.

Abbreviations

AD: Alzheimer's disease; ANOVA: analysis of variance; AP: amyloid plaques; BA: Brodmann area; DLB: dementia with Lewy bodies; FDR: false discovery rate; FynB: Fyn kinase isoform B; FynT: Fyn kinase isoform T; GO: Gene Ontology; HTA: Human Transcriptome Array; LB: Lewy bodies; MMSE: Mini-Mental State Examination; NFT: neurofibrillary tangles; PDD: Parkinson's disease dementia; RT-PCR: real-time polymerase chain reaction; sA β 42: soluble fraction of β -amyloid₁₋₄₂ peptide.

Funding

This work was supported by a research grant (NMRC/OFIRG/0028/2016) to MGKT and MKPL by the National Medical Research Council, Singapore.

Authors' Contributions

MGKT and MKPL conceived the study and designed the project; CYBL, JHL, FWTL, CL performed the experiments; DA, CB, PTF provided postmortem and clinical data; CYBL, JHL, MGKT analyzed the data; MGKT, MKPL wrote the first draft. All authors have read and approved the manuscript.

Ethics approval and consent to participate

For the postmortem study, ethics approval for the collection and study of brain tissues received Institutional Review Board approval in both the UK (08/H1010/4) and Singapore institutions (NUS 12-062E), and informed consent was obtained from participants' next-of-kin prior to removal of brain. The mice studies were approved

by the SingHealth Group Institutional Animal Care and Use Committee
(2017/SHS/1280).

Consent for publication

All authors gave consent for publication.

Competing interests

The authors declare that they have no competing interests.

References

1. Aarsland D, Ballard CG, Halliday G (2004) Are Parkinson's disease with dementia and dementia with Lewy bodies the same entity? *J Geriatr Psychiatry Neurol.*17(3):137-45.
2. Alghamdi A, Vallortigara J, Howlett DR, Broadstock M, Hortobagyi T, Ballard C, Thomas AJ, O'Brien JT, Aarsland D, Attems J, Francis PT, Whitfield DR (2017) Reduction of RPT6/S8 (a Proteasome Component) and Proteasome Activity in the Cortex is Associated with Cognitive Impairment in Lewy Body Dementia. *Journal of Alzheimer's disease : JAD.*57(2):373-86.
3. Alves LCS, Monteiro DQ, Bento SR, Hayashi VD, Pelegrini LNC, Vale FAC (2019) Burnout syndrome in informal caregivers of older adults with dementia: A systematic review. *Dement Neuropsychol.*13(4):415-21.
4. Ballard CG, Aarsland D, McKeith I, O'Brien J, Gray A, Cormack F, Burn D, Cassidy T, Starfeldt R, Larsen JP, Brown R, Tovee M (2002) Fluctuations in attention: PD dementia vs DLB with parkinsonism. *Neurology.*59(11):1714-20.
5. Benjamini Y, Hochberg Y (2008) Controlling the false discovery rate: a practical and powerful approach to multiple testing. *J R Statist Soc B.*57(1):289-300.
6. Bennett DA, Schneider JA, Wilson RS, Bienias JL, Arnold SE (2004) Neurofibrillary tangles mediate the association of amyloid load with clinical Alzheimer disease and level of cognitive function. *Arch Neurol.*61(3):378-84.
7. Braak H, Braak E (1991) Neuropathological staging of Alzheimer-related changes. *Acta neuropathologica.*82(4):239-59.
8. Braak H, Del Tredici K (2018) Spreading of Tau Pathology in Sporadic Alzheimer's Disease Along Cortico-cortical Top-Down Connections. *Cerebral cortex.*28(9):3372-84.
9. Calsolaro V, Edison P (2016) Neuroinflammation in Alzheimer's disease: Current evidence and future directions. *Alzheimer's & dementia : the journal of the Alzheimer's Association.*12(6):719-32.
10. Chai YL, Chong JR, Weng J, Howlett D, Halsey A, Lee JH, Attems J, Aarsland D, Francis PT, Chen CP, Lai MKP (2019) Lysosomal cathepsin D is upregulated in Alzheimer's disease neocortex and may be a marker for neurofibrillary degeneration. *Brain pathology.*29(1):63-74.
11. Chin J, Palop JJ, Puolivali J, Massaro C, Bien-Ly N, Gerstein H, Scearce-Levie K, Masliah E, Mucke L (2005) Fyn kinase induces synaptic and cognitive impairments in a transgenic mouse model of Alzheimer's disease. *The Journal of neuroscience : the official journal of the Society for Neuroscience.*25(42):9694-703.
12. Chin J, Palop JJ, Yu GQ, Kojima N, Masliah E, Mucke L (2004) Fyn kinase modulates synaptotoxicity, but not aberrant sprouting, in human amyloid precursor protein transgenic mice. *The Journal of neuroscience : the official journal of the Society for Neuroscience.*24(19):4692-7.
13. Edison P, Rowe CC, Rinne JO, Ng S, Ahmed I, Kempainen N, Villemagne VL, O'Keefe G, Nagren K, Chaudhury KR, Masters CL, Brooks DJ (2008) Amyloid load in Parkinson's disease dementia and Lewy body dementia measured with [¹¹C]PIB positron emission tomography. *J Neurol Neurosurg Psychiatry.*79(12):1331-8.
14. Eng LF, Ghirnikar RS (1994) GFAP and astrogliosis. *Brain pathology.*4(3):229-37.
15. Folstein MF, Folstein SE, McHugh PR (1975) "Mini-mental state". A practical method for grading the cognitive state of patients for the clinician. *J Psychiatr Res.*12(3):189-98.
16. Francis PT, Perry EK (2007) Cholinergic and other neurotransmitter mechanisms in Parkinson's disease, Parkinson's disease dementia, and dementia with Lewy bodies. *MovDisord.*22 Suppl 17:S351-S7.
17. Fujiwara H, Hasegawa M, Dohmae N, Kawashima A, Masliah E, Goldberg MS, Shen J, Takio K, Iwatsubo T (2002) a-Synuclein is phosphorylated in synucleinopathy lesions. *Nat Cell Biol.*4(2):160-4.

18. Gomperts SN, Locascio JJ, Makaretz SJ, Schultz A, Caso C, Vasdev N, Sperling R, Growdon JH, Dickerson BC, Johnson K (2016) Tau Positron Emission Tomographic Imaging in the Lewy Body Diseases. *JAMA Neurol.*73(11):1334-41.
19. Gomperts SN, Locascio JJ, Marquie M, Santarlasci AL, Rentz DM, Maye J, Johnson KA, Growdon JH (2012) Brain amyloid and cognition in Lewy body diseases. *Movement disorders : official journal of the Movement Disorder Society.*27(8):965-73.
20. Haass C, Mandelkow E (2010) Fyn-tau-amyloid: a toxic triad. *Cell.*142(3):356-8.
21. Hansen DV, Hanson JE, Sheng M (2018) Microglia in Alzheimer's disease. *The Journal of cell biology.*217(2):459-72.
22. Hepp DH, Vergoossen DL, Huisman E, Lemstra AW, Berendse HW, Rozemuller AJ, Foncke EM, van de Berg WD (2016) Distribution and Load of Amyloid-beta Pathology in Parkinson Disease and Dementia with Lewy Bodies. *Journal of neuropathology and experimental neurology.*75(10):936-45.
23. Howlett DR, Whitfield D, Johnson M, Attems J, O'Brien JT, Aarsland D, Lai MK, Lee JH, Chen C, Ballard C, Hortobágyi T, Francis PT (2015) Regional multiple pathology scores are associated with cognitive decline in Lewy body Dementias. *Brain pathology.*25(4):401-8.
24. Huang da W, Sherman BT, Lempicki RA (2009) Bioinformatics enrichment tools: paths toward the comprehensive functional analysis of large gene lists. *Nucleic acids research.*37(1):1-13.
25. Huang da W, Sherman BT, Lempicki RA (2009) Systematic and integrative analysis of large gene lists using DAVID bioinformatics resources. *Nature protocols.*4(1):44-57.
26. Huang DW, Sherman BT, Lempicki RA (2009) Systematic and integrative analysis of large gene lists using DAVID bioinformatics resources. *Nature protocols.*4(1):44-57.
27. Hurd MD, Martorell P, Delavande A, Mullen KJ, Langa KM (2013) Monetary costs of dementia in the United States. *N Engl J Med.*368(14):1326-34.
28. Ittner LM, Ke YD, Delerue F, Bi M, Gladbach A, van Eersel J, Wolfing H, Chieng BC, Christie MJ, Napier IA, Eckert A, Staufenbiel M, Hardeman E, Götz J (2010) Dendritic function of tau mediates amyloid-b toxicity in Alzheimer's disease mouse models. *Cell.*142(3):387-97.
29. Jellinger KA, Korczyn AD (2018) Are dementia with Lewy bodies and Parkinson's disease dementia the same disease? *BMC Med.*16(1):34.
30. Kaufman AC, Salazar SV, Haas LT, Yang J, Kostylev MA, Jeng AT, Robinson SA, Gunther EC, van Dyck CH, Nygaard HB, Strittmatter SM (2015) Fyn inhibition rescues established memory and synapse loss in Alzheimer mice. *Annals of neurology.*77(6):953-71.
31. Larson M, Sherman MA, Amar F, Nuvolone M, Schneider JA, Bennett DA, Aguzzi A, Lesne SE (2012) The complex PrP(c)-Fyn couples human oligomeric Abeta with pathological tau changes in Alzheimer's disease. *The Journal of neuroscience : the official journal of the Society for Neuroscience.*32(47):16857-71a.
32. Lau DH, Hogseth M, Phillips EC, O'Neill MJ, Pooler AM, Noble W, Hanger DP (2016) Critical residues involved in tau binding to fyn: implications for tau phosphorylation in Alzheimer's disease. *Acta neuropathologica communications.*4(1):49.
33. Laurent C, Buee L, Blum D (2018) Tau and neuroinflammation: What impact for Alzheimer's Disease and Tauopathies? *Biomed J.*41(1):21-33.
34. Lee C, Low CY, Francis PT, Attems J, Wong PT, Lai MK, Tan MG (2016) An isoform-specific role of FynT tyrosine kinase in Alzheimer's disease. *Journal of neurochemistry.*136(3):637-50.
35. Lee C, Low CY, Wong SY, Lai MK, Tan MG (2017) Selective induction of alternatively spliced FynT isoform by TNF facilitates persistent inflammatory responses in astrocytes. *Sci Rep.*7:43651.
36. Lee G, Thangavel R, Sharma VM, Litersky JM, Bhaskar K, Fang SM, Do LH, Andreadis A, Van HG, Ksiezak-Reding H (2004) Phosphorylation of tau by fyn: implications for Alzheimer's

disease. *The Journal of neuroscience : the official journal of the Society for Neuroscience*.24(9):2304-12.

37. Li C, Gotz J (2017) Somatodendritic accumulation of Tau in Alzheimer's disease is promoted by Fyn-mediated local protein translation. *The EMBO journal*.36(21):3120-38.

38. Ling EA, Wong WC (1993) The origin and nature of ramified and amoeboid microglia: a historical review and current concepts. *Glia*.7(1):9-18.

39. Lippa CF, Duda JE, Grossman M, Hurtig HI, Aarsland D, Boeve BF, Brooks DJ, Dickson DW, Dubois B, Emre M, Fahn S, Farmer JM, Galasko D, Galvin JE, Goetz CG, Growdon JH, Gwinn-Hardy KA, Hardy J, Heutink P, Iwatsubo T, Kosaka K, Lee VM, Leverenz JB, Masliah E, McKeith IG, Nussbaum RL, Olanow CW, Ravina BM, Singleton AB, Tanner CM, Trojanowski JQ, Wszolek ZK (2007) DLB and PDD boundary issues: diagnosis, treatment, molecular pathology, and biomarkers. *Neurology*.68(11):812-9.

40. McKeith IG, Dickson DW, Lowe J, Emre M, O'Brien JT, Feldman H, Cummings J, Duda JE, Lippa C, Perry EK, Aarsland D, Arai H, Ballard CG, Boeve B, Burn DJ, Costa D, Del ST, Dubois B, Galasko D, Gauthier S, Goetz CG, Gomez-Tortosa E, Halliday G, Hansen LA, Hardy J, Iwatsubo T, Kalaria RN, Kaufer D, Kenny RA, Korczyn A, Kosaka K, Lee VM, Lees A, Litvan I, Londos E, Lopez OL, Minoshima S, Mizuno Y, Molina JA, Mukaetova-Ladinska EB, Pasquier F, Perry RH, Schulz JB, Trojanowski JQ, Yamada M (2005) Diagnosis and management of dementia with Lewy bodies: third report of the DLB Consortium. *Neurology*.65(12):1863-72.

41. Metcalfe MJ, Figueiredo-Pereira ME (2010) Relationship between tau pathology and neuroinflammation in Alzheimer's disease. *The Mount Sinai journal of medicine, New York*.77(1):50-8.

42. Minter MR, Taylor JM, Crack PJ (2016) The contribution of neuroinflammation to amyloid toxicity in Alzheimer's disease. *J Neurochem*.136(3):457-74.

43. Mohamed NE, Howlett DR, Ma L, Francis PT, Aarsland D, Ballard CG, McKeith IG, Chen CP, Lai MK (2014) Decreased immunoreactivities of neocortical AMPA receptor subunits correlate with motor disability in Lewy body dementias. *J Neural Transm (Vienna)*.121(1):71-8.

44. Nelson PT, Alafuzoff I, Bigio EH, Bouras C, Braak H, Cairns NJ, Castellani RJ, Crain BJ, Davies P, Del Tredici K, Duyckaerts C, Frosch MP, Haroutunian V, Hof PR, Hulette CM, Hyman BT, Iwatsubo T, Jellinger KA, Jicha GA, Kovari E, Kukull WA, Leverenz JB, Love S, Mackenzie IR, Mann DM, Masliah E, McKee AC, Montine TJ, Morris JC, Schneider JA, Sonnen JA, Thal DR, Trojanowski JQ, Troncoso JC, Wisniewski T, Woltjer RL, Beach TG (2012) Correlation of Alzheimer disease neuropathologic changes with cognitive status: a review of the literature. *Journal of neuropathology and experimental neurology*.71(5):362-81.

45. Nygaard HB (2018) Targeting Fyn Kinase in Alzheimer's Disease. *Biological psychiatry*.83(4):369-76.

46. Padmanabhan P, Martinez-Marmol R, Xia D, Gotz J, Meunier FA (2019) Frontotemporal dementia mutant Tau promotes aberrant Fyn nanoclustering in hippocampal dendritic spines. *eLife*.8.

47. Panicker N, Saminathan H, Jin H, Neal M, Harischandra DS, Gordon R, Kanthasamy K, Lawana V, Sarkar S, Luo J, Anantharam V, Kanthasamy AG, Kanthasamy A (2015) Fyn Kinase Regulates Microglial Neuroinflammatory Responses in Cell Culture and Animal Models of Parkinson's Disease. *The Journal of neuroscience : the official journal of the Society for Neuroscience*.35(27):10058-77.

48. Panicker N, Sarkar S, Harischandra DS, Neal M, Kam TI, Jin H, Saminathan H, Langley M, Charli A, Samidurai M, Rokad D, Ghaisas S, Pletnikova O, Dawson VL, Dawson TM, Anantharam V, Kanthasamy AG, Kanthasamy A (2019) Fyn kinase regulates misfolded alpha-synuclein uptake and NLRP3 inflammasome activation in microglia. *The Journal of experimental medicine*.216(6):1411-30.

49. Reitz C (2012) Alzheimer's disease and the amyloid cascade hypothesis: a critical review. *International journal of Alzheimer's disease*.2012:369808.
50. Resh MD (1998) Fyn, a Src family tyrosine kinase. *The international journal of biochemistry & cell biology*.30(11):1159-62.
51. Sharma P, Srivastava P, Seth A, Tripathi PN, Banerjee AG, Shrivastava SK (2019) Comprehensive review of mechanisms of pathogenesis involved in Alzheimer's disease and potential therapeutic strategies. *Progress in neurobiology*.174:53-89.
52. Surendranathan A, Rowe JB, O'Brien JT (2015) Neuroinflammation in Lewy body dementia. *Parkinsonism Relat Disord*.21(12):1398-406.
53. Trepanier CH, Jackson MF, MacDonald JF (2012) Regulation of NMDA receptors by the tyrosine kinase Fyn. *The FEBS journal*.279(1):12-9.
54. Tsuboi Y, Dickson DW (2005) Dementia with Lewy bodies and Parkinson's disease with dementia: are they different? *Parkinsonism Relat Disord*.11 Suppl 1:S47-51.
55. Um JW, Nygaard HB, Heiss JK, Kostylev MA, Stagi M, Vortmeyer A, Wisniewski T, Gunther EC, Strittmatter SM (2012) Alzheimer amyloid-beta oligomer bound to postsynaptic prion protein activates Fyn to impair neurons. *Nature neuroscience*.15(9):1227-35.
56. van Dyck CH, Nygaard HB, Chen K, Donohue MC, Raman R, Rissman RA, Brewer JB, Koeppe RA, Chow TW, Rafii MS, Gessert D, Choi J, Turner RS, Kaye JA, Gale SA, Reiman EM, Aisen PS, Strittmatter SM (2019) Effect of AZD0530 on Cerebral Metabolic Decline in Alzheimer Disease: A Randomized Clinical Trial. *JAMA neurology*.
57. Wang H, Ren CH, Gunawardana CG, Schmitt-Ulms G (2013) Overcoming barriers and thresholds - signaling of oligomeric Abeta through the prion protein to Fyn. *Molecular neurodegeneration*.8:24.
58. Whitfield DR, Vallortigara J, Alghamdi A, Howlett D, Hortobagyi T, Johnson M, Attems J, Newhouse S, Ballard C, Thomas AJ, O'Brien JT, Aarsland D, Francis PT (2014) Assessment of ZnT3 and PSD95 protein levels in Lewy body dementias and Alzheimer's disease: association with cognitive impairment. *Neurobiol Aging*.35(12):2836-44.
59. Xing H, Lim YA, Chong JR, Lee JH, Aarsland D, Ballard CG, Francis PT, Chen CP, Lai MK (2016) Increased phosphorylation of collapsin response mediator protein-2 at Thr514 correlates with b-amyloid burden and synaptic deficits in Lewy body dementias. *Mol Brain*.9(1):84.
60. Yoshiyama Y, Higuchi M, Zhang B, Huang SM, Iwata N, Saido TC, Maeda J, Suhara T, Trojanowski JQ, Lee VM (2007) Synapse loss and microglial activation precede tangles in a P301S tauopathy mouse model. *Neuron*.53(3):337-51.
61. Zweig YR, Galvin JE (2014) Lewy body dementia: the impact on patients and caregivers. *Alzheimer's research & therapy*.6(2):21.

Table 1. Demographic and disease variables of a cohort of patients with neuropathologically confirmed AD and LBD

Demographics [¶]		Control (n=16)	AD (n=13)	DLB (n=39)	PDD (n=27)
<i>Gender (male/ female)</i>		9M/ 7F	5M/ 8F	26M/ 13F	15M/ 12F
<i>Age at death (years)</i>		82.0 ± 1.7	86.1 ± 1.9	80.9 ± 1.1	79.3 ± 1.2
<i>Postmortem interval (hours)</i>		45.7 ± 5.9	36.7 ± 7.1	43.7 ± 4.9	33.5 ± 3.0
<i>MMSE before death</i>		-	9 ± 2.1 (n=13)	14 ± 1.5 (n=32)	12 ± 1.6 (n=25)
<i>Braak staging</i>	<i>0-II</i>	11 (91.7%)	0 (0%)	6 (15.4%)	18 (66.7%)
	<i>III-IV</i>	1 (8.3%)	3 (23%)	20 (51.3%)	7 (26%)
	<i>V-VI</i>	0 (0%)	10 (77%)	13 (33.3%)	2 (7.3%)
ELISA assay					
<i>soluble Aβ42 (pg/mg)(BA9)</i>		5.6 ± 1.5 (n=15)	33.2 ± 2.2* (n=13)	29.6 ± 2.4* (n=37)	10.9 ± 1.8^# (n=26)
<i>soluble Aβ42 (pg/mg) (BA21)</i>		6.2 ± 1.5 (n=15)	27.5 ± 2.4* (n=13)	25.2 ± 1.9* (n=39)	10.3 ± 1.8^# (n=26)
<i>pS396Tau (pg/mg) (BA9)</i>		5.4 ± 2.7 (n=16)	168.4 ± 33.3* (n=13)	47.6 ± 13.8^ (n=39)	2.2 ± 0.6^# (n=27)
<i>pS396Tau (pg/mg) (BA21)</i>		25.1 ± 5.6 (n=15)	524.8 ± 92.9* (n=13)	215.1 ± 48^ (n=38)	61.9 ± 25.6^ (n=26)

Data are presented as mean ± S.E.M.

[¶]Maximum available n. Not all samples were available for all assessments. Available n listed in individual assessments.

*Significantly different compared to CTRL (one-way ANOVA with Bonferroni *post-hoc*, $p < 0.05$)

^Significantly different compared to AD (one-way ANOVA with Bonferroni *post-hoc*, $p < 0.05$)

[§]Significantly different compared to DLB (one-way ANOVA with Bonferroni *post-hoc*, $p < 0.05$)

Table 2. Top five* GO Terms under BP and CC categories for FynT positively- and negatively-correlated genes

GO Term ID (Categories)	Description (FynT positively correlated genes)	Count^a	Fold Enrichment^b	Benjamini^c
GO:0005913 (CC)	cell-cell adherens junction	34	4.07	2.64E-09
GO:0005925 (CC)	focal adhesion	37	3.66	4.69E-09
GO:0030027 (CC)	lamellipodium	18	4.35	5.62E-05
GO:0030175 (CC)	filopodium	12	6.54	9.64E-05
GO:0001726 (CC)	ruffle	13	5.59	1.53E-04
GO:0098609 (BP)*	cell-cell adhesion	24	3.23	4.00E-03
GO:0016569 (BP)*	covalent chromatin modification	14	4.51	1.52E-02
GO Term ID (Categories)	Description (FynT negatively correlated genes)	Count^a	Fold Enrichment^b	Benjamini^c
GO:0043209 (CC)	myelin sheath	54	4.75	3.64E-20
GO:0030054 (CC)	cell junction	91	2.65	1.62E-15
GO:0014069 (CC)	postsynaptic density	50	3.64	2.66E-13
GO:0008021 (CC)	synaptic vesicle	33	4.80	5.41E-12
GO:0045211 (CC)	postsynaptic membrane	49	3.11	2.28E-10
GO:0016192 (BP)	vesicle-mediated transport	40	3.41	2.46E-08
GO:0034220 (BP)	ion transmembrane transport	48	2.96	2.57E-08
GO:0006886 (BP)	intracellular protein transport	52	2.85	4.34E-08
GO:0000165 (BP)	MAPK cascade	54	2.67	6.03E-08
GO:0016241 (BP)	regulation of macroautophagy	20	5.88	1.06E-07

Gene ontology (GO) category: biological process (BP) and cellular component (CC)

*For FynT positively correlated genes, only two BP terms were significant at FDR < 0.05.

^aCount represents the total number of gens correlated with FynT in the respective GO term.

^bFold enrichment is used to measure the magnitude of enrichment.

^c*p*-values adjusted for multiple testing using FDR < 0.05.

Figure Legends

Fig. 1 Specific up-regulation of FynT isoform expression in prefrontal cortex of AD and LBD. Gene View plot demonstrates differential alternative splicing of Fyn in BA9 samples of CTRL (n=9, red), AD (n=9, blue), DLB (n=12, amber) and PDD (n=12, green), from data derived from Affymetrix HTA array. Light blue asterisk indicated the PSR06025242.hg.1 probeset, with a magnified view shown in the inset, corresponding to the FynT-specific exon highlighted in blue. FynB-specific exons are highlighted in yellow. The Y-axis is in Log₂ scale intensity value. The *p* values shown are of Alt-splicing ANOVAs using the Partek Genomic Suite® software.

Fig. 2 Increased FynT to FynB ratios in prefrontal and temporal cortex of AD and LBD.

A Representative electropherograms of the proportional levels of FynB and FynT in each sample as determined by RT-PCR using common primers spanning the alternatively spliced exon of Fyn followed by capillary electrophoresis. Relative fluorescence units (RFU) of FynT peak (219bp DNA amplicon) and FynB peak (128bp DNA amplicon) are shown for each diagnostic group. **B** Peak areas of FynT and FynB in each electropherogram were converted to gene transcript levels and used to determine ratio of FynT to FynB expression, depicted as dot plots of CTRL (n=14, red), AD (n=13, red), DLB (n=18, amber) and PDD (n=19, green) values with horizontal lines in each group indicating median and interquartile range.

p*<0.05, *p*<0.01, ****p*<0.001, Significantly different from CTRL by Kruskal-Wallis ANOVA with *post-hoc* Dunn's tests.

Fig. 3 FynT upregulation in AD and LBD correlates with cognitive impairment and neuropathological features. **A** FynT and FynB expression were determined by real-time RT-PCR in BA9 and BA21, derived from CTRL (n=13-15, red), AD (n=11-12, blue), DLB (n=25-31, amber) and PDD (n=14-21, green). Data were Log₂ transformed and depicted as box plots, with the horizontal intersecting lines and borders indicating median and interquartile range for each group, while whiskers show the highest and lowest values not considered outliers. **B** Scatter plots of Log₂-transformed FynT expression against pre-death cognition (MMSE) scores in BA9 (left) and BA21 (right) in the combined dementia cohort. Solid lines indicated linear regressed best-fit curves while dashed lines indicated their respective 95% confidence intervals, with insets showing Pearson's correlation coefficients (r) and their respective p values. **C** Table of correlation coefficients for FynT or FynB expression with neuropathologic scores, Braak stage and biochemical measures of pS396Tau and soluble Aβ42 (in pg/mg protein).

p<0.01, *p<0.001, significant differences compared to CTRL by one-way ANOVA with *post-hoc* Bonferroni's tests.

[¶]Pearson's (r) and [§]Spearman's (ρ) correlation coefficients with p < 0.05.

Fig. 4 Association of FynT expression with neuroinflammatory markers in AD and LBD. **A** Gene expression of GFAP astrocytic marker (left) and CD11b microglial marker (right) were determined by real-time RT-PCR in BA9 and BA21, derived from CTRL (n=13-15, red), AD (n=11-12, blue), DLB (n=25-31, amber) and PDD (n=14-21, green). Data were Log₂ transformed and depicted as box plots, with the horizontal intersecting lines and borders indicating median and interquartile range for each

group, while whiskers show the highest and lowest values not considered outliers. **B** Scatter plots of Log₂-transformed FynT expression against GFAP (left) and CD11b (right) in BA9 (top) and BA21 (bottom) of the combined cohort. Solid lines indicated linear regressed best-fit curves while dashed lines indicated their respective 95% confidence intervals, with insets showing Pearson's correlation coefficients (*r*) and their respective *p* values.

p*<0.05, *p*<0.01, ****p*<0.001, significant pairwise differences between diagnostic groups by one-way ANOVA with *post-hoc* Bonferroni's tests.

Fig. 5 Selective upregulation of FynT in aged transgenic P301S tau mice correlates with tauopathy and neuroinflammation. **A** Determination of phosphorylated tau (pS202/T205 tau), aggregated tau and total tau protein by HTRF in the brain homogenates of P301S Tau transgenic mice and wildtype littermate controls at age < 6 mo (before onset of pathology, labels in small letters: p301s, wt) and ≥ 6 mo (with disease progression, labels in capital letters: P301S, WT). RT-PCR derived values for relative expressions of **B** FynT, FynB (together with FynT to FynB ratios) as well as **C** GFAP and CD11b in the samples as described above. **D** Table of correlation coefficients for FynT, FynB, FynT:FynB with phosphorylated tau, aggregated tau, and neuroinflammation markers.

p*<0.05, *p*<0.01, ****p*<0.001, significant pairwise differences between diagnostic groups by one-way ANOVA with *post-hoc* Bonferroni's tests.

[†]Pearson's (*r*) correlation coefficients with *p* < 0.05.

Figure 1. Specific up-regulation of FynT isoform expression in prefrontal cortex of AD and LBD

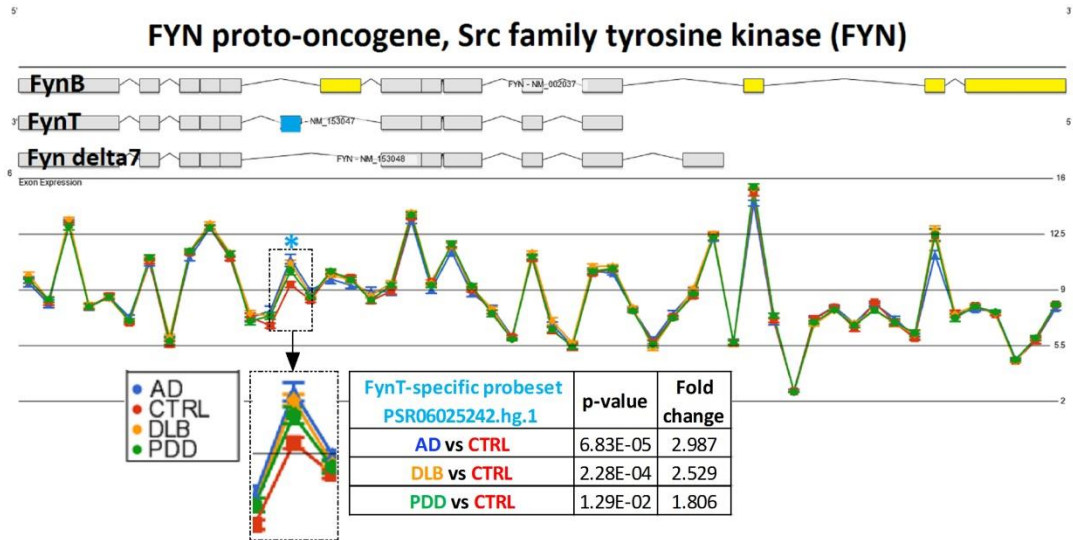


Figure 2. Increased FynT to FynB ratios in prefrontal and temporal cortex of AD and LBD

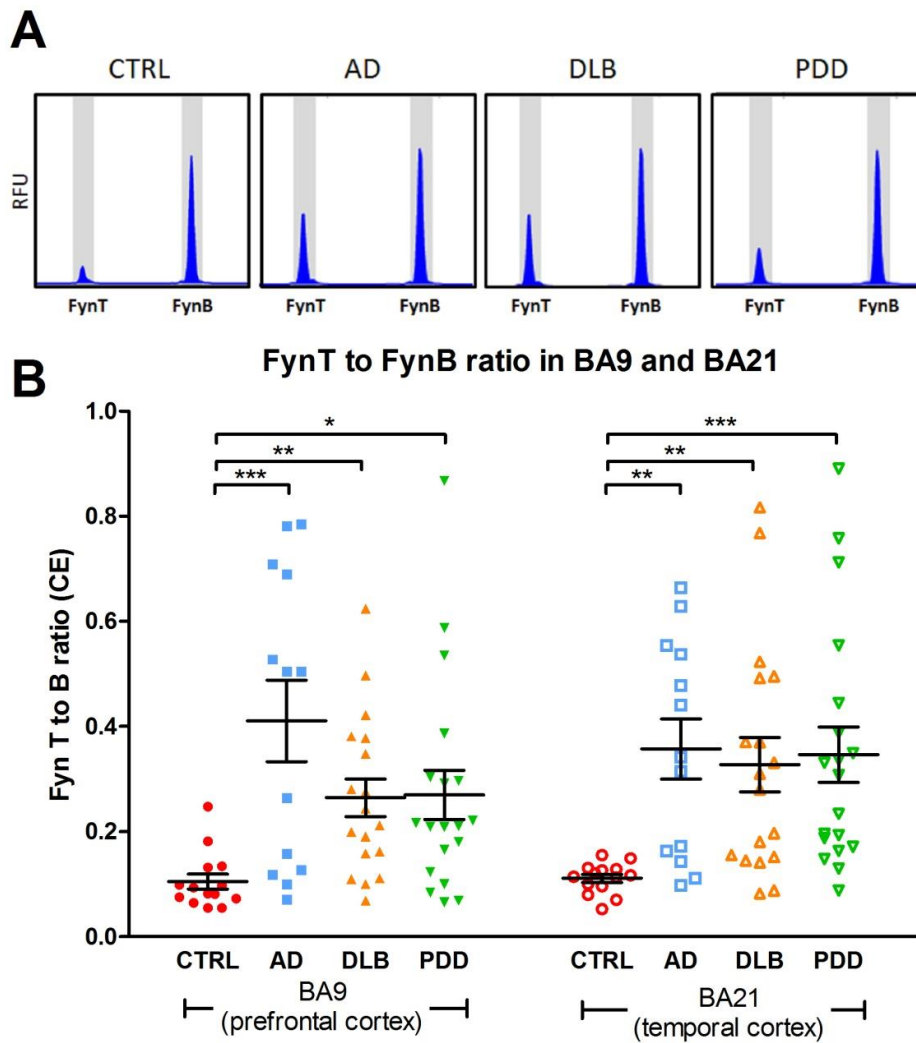


Figure 3. FynT upregulation in AD and LBD correlates with cognitive impairment and neuropathological features

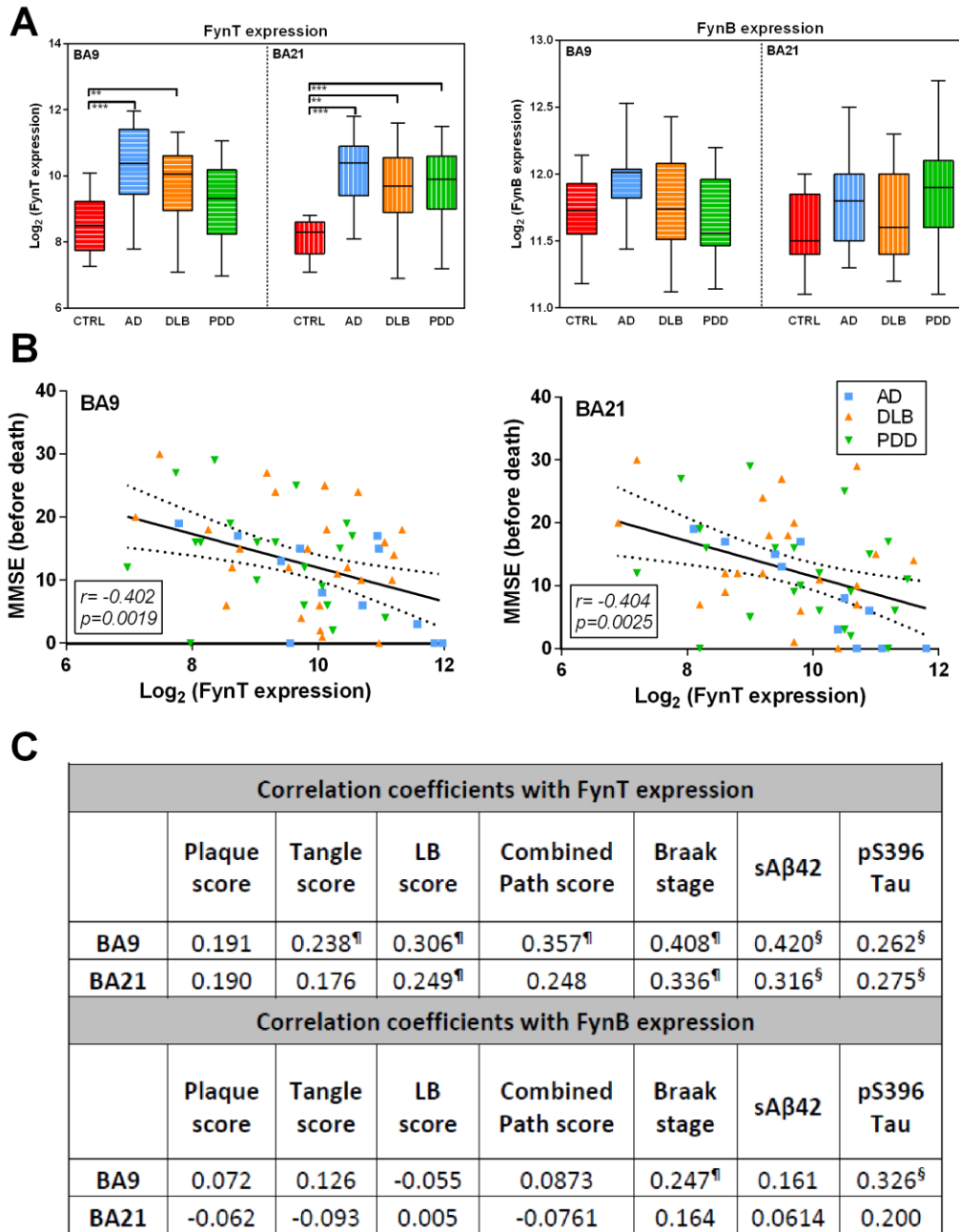


Figure 4. Association of FynT expression with neuroinflammatory markers in AD and LBD

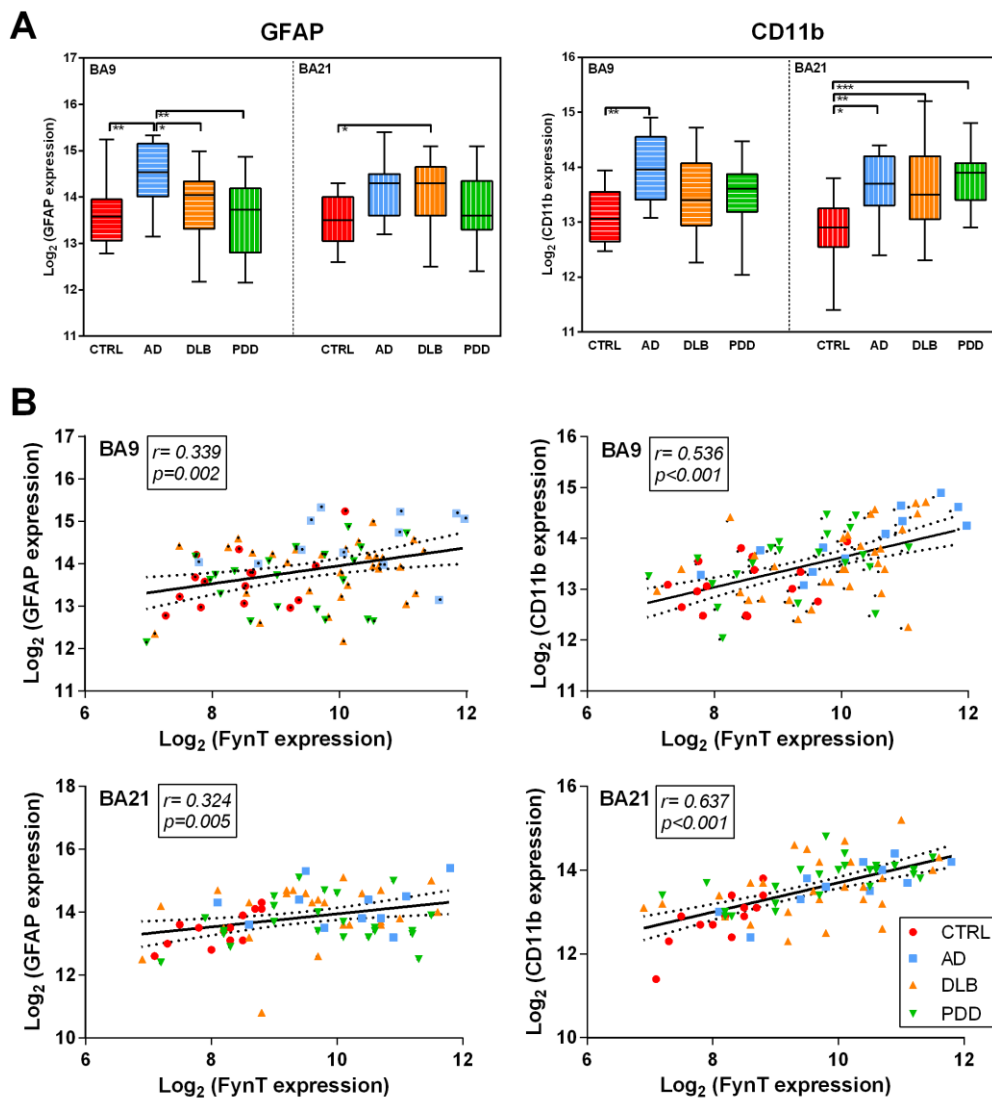
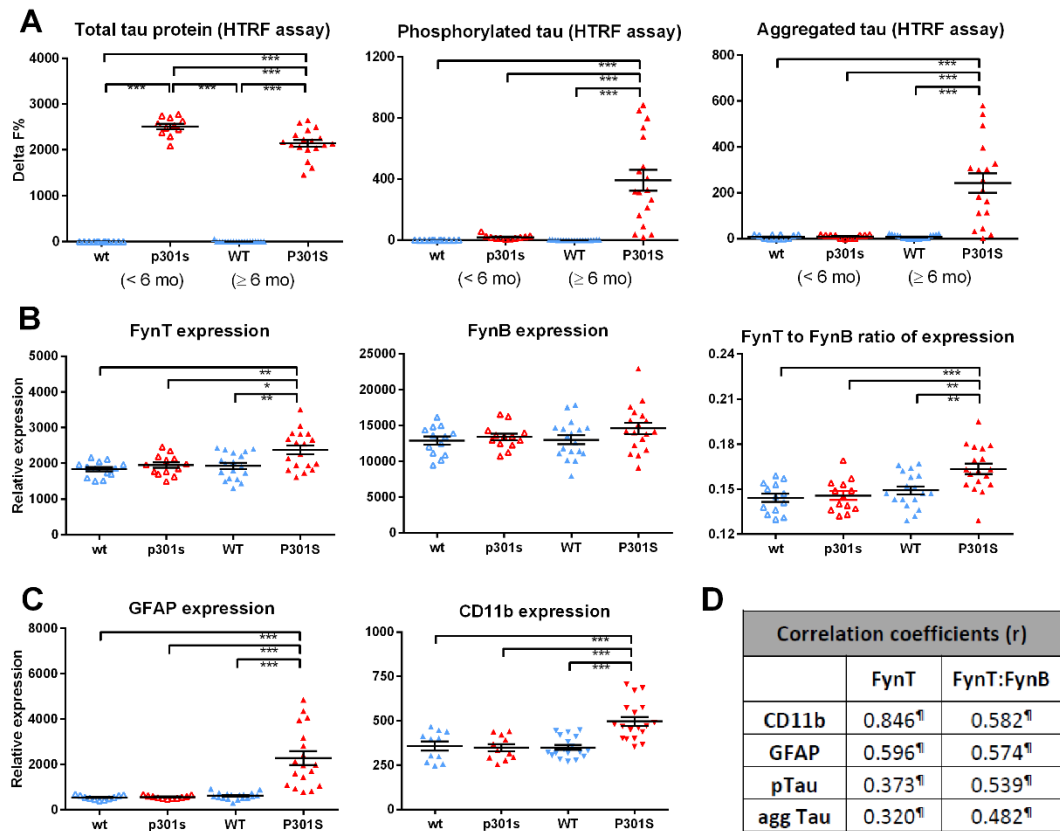


Figure 5. Selective upregulation of FynT in aged transgenic P301S tau mice correlates with tauopathy and neuroinflammation



Supplementary Table S1. Primers used in the real-time RT-PCR

Primer Name	Forward primer seq (5'-3')	Reverse primer seq (5'-3')	Accession no (product size)
Hs_FynB	CTGCTGCCGCCTAGTAGTTC	GTGTTTCCATTCCAGGTACC	NM_002037 (168bp)
Hs_FynT	CATCGAGTTGTACCCACAA	GTGTTTCCATTCCAGGTACC	NM_153047 (136bp)
Hs_GFAP	GGGAGCTTGATTCTCAGCAC	AATTGCCCTCCTCCATCT	NM_002055 (178bp)
Hs_CD11b	GCCGGTGAAATATGCTGTCT	GCGGTCCCATATGACAGTCT	NM_001145808 (199bp)
Hs_18S rRNA	CCTGCGGCTTAATTTGACTC	CGCTGAGCCAGTCAGTGTAG	M10098 (310bp)
Hs_β-actin	ACTGGAACGGTGAAGGTGAC	AGAGAAGTGGGGTGGCTTTT	NM_001101 (169bp)
Hs_GAPDH	TGACATCAAGAAGGTGGTGAAG	TTACTCCTTGAGAGCCATGTG	M33197 (241bp)
Ms FynB	CTGCTGCCGCCTAGTAGTTC	GTATTTCCATTCCAGGTACC	NM_001122893 (168bp)
Ms FynT	CATCAAGTTGTACCCACAA	GTATTTCCATTCCAGGTACC	NM_008054 (136bp)
Ms GFAP	TGAGGCAGAAGCTCCAAGAT	CACGTGGACCTGCTGTTG	NM_001131020 (215bp)
Ms CD11b	CAGCATCAGTACCAGTTCACAA	CTGCAACAGAGCAGTTCAGC	NM_001082960 (223bp)
Ms 18S rRNA	CCTGCGGCTTAATTTGACTC	CGCTGAGCCAGTCAGTGTAG	NR_003278 (319bp)
Ms GAPDH	GGCATTGCTCTCAATGACAA	TGTGAGGGAGATGCTCAGTG	NM_008084 (200bp)
Ms β-actin	ACTGGAACGGTGAAGGCGAC	GAGGGTGAGGGACTTCCTGT	NM_007393 (175bp)

(* indicate Fyn primer sets for fragment analysis using capillary electrophoresis, with 5' labeled 6-FAM on reverse primer)

Supplementary Figure S1

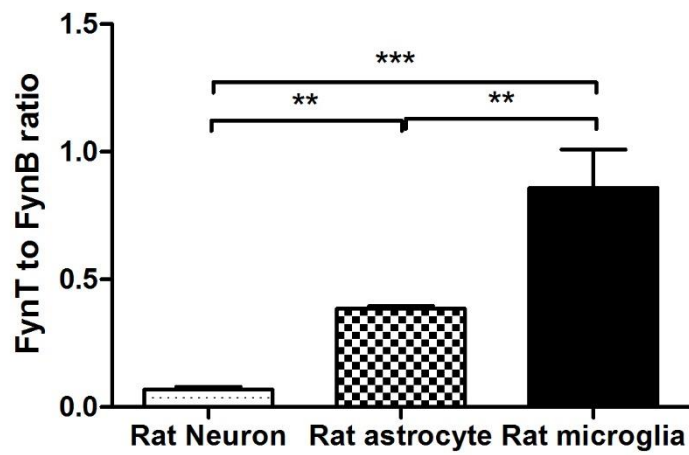


Figure S1. Higher proportions of FynT expression in rat primary microglia cells. Endogenous FynT to FynB ratios were determined by RT-PCR followed by CE (see Methods) in primary neurons, astrocytes and microglia cells. Data are mean \pm S.E.M of N = 3 - 6 independent isolations of each primary culture.

** $p < 0.01$, *** $p < 0.001$, significant pairwise differences between diagnostic groups by one-way ANOVA with *post-hoc* Bonferroni's tests.